Thermochimica Acta, 217 (1993) 241–249
Elsevier Science Publishers B.V., Amsterdam

Thermoanalysis of the system BaO_2–BaO–O_2

A.F. Mayorova *, S.N. Mudretsova, M.N. Mamontov, P.A. Levashov and A.D. Rusin

Department of Chemistry, Moscow State University, Moscow GSP 119899 (Russian Federation)

(Received 26 June 1992)

Abstract

Thermoanalysis of the system BaO_2–BaO–O_2 has been carried out at oxygen pressures from 0.2 to 1.5 atmospheres using a Netzsch STA-409 simultaneous analyser. Measurements were made over the temperature range from 25 to 950°C. The thermogravimetric data obtained have been used to evaluate the non-stoichometric region boundaries for BaO_2 and to estimate the same region for BaO. The temperatures of the monovariant equilibrium BaO_{1+x_1}–BaO_{2-x_2} have been determined: $T_{mon} = 990$, 1041, 1083 and 1109 K at $P_{O_2} = 0.2$, 0.5, 1.0 and 1.5 oxygen atmospheres, respectively. For the reaction $BaO_{1.0} + 0.5O_2 = BaO_{2.0}$, the values $\Delta G_T^{\ominus} = -5.1$, -2.1, 0.3, and 1.7 kJ mol^{-1} have been calculated for the above respective temperatures.

INTRODUCTION

The study of the thermal behaviour of BaO_2 and BaO over a wide range of temperatures and oxygen pressures is of significance because of their role in the formation and degradation of ceramic superconductors.

The system BaO_2–BaO–O_2 has been investigated in a number of studies [1–9]. The experimental study of the oxides is rather difficult because of their high reactivity. There are some mistakes in earlier papers [1–4]. For example before the publication of ref. 6, BaO_2 was erroneously believed to be formed only in the presence of water vapour. The study in ref. 6 was performed in an atmosphere of dry oxygen and the composition of the preparation was determined in changing pressure under isothermal conditions. The data obtained enabled the dependence of the solution compositions on equilibrium pressure in divariant regions, as well as the dependences of the solution composition on pressure and temperature in a monovariant region, to be expressed in analytical form. In a subsequent

---

* Corresponding author.

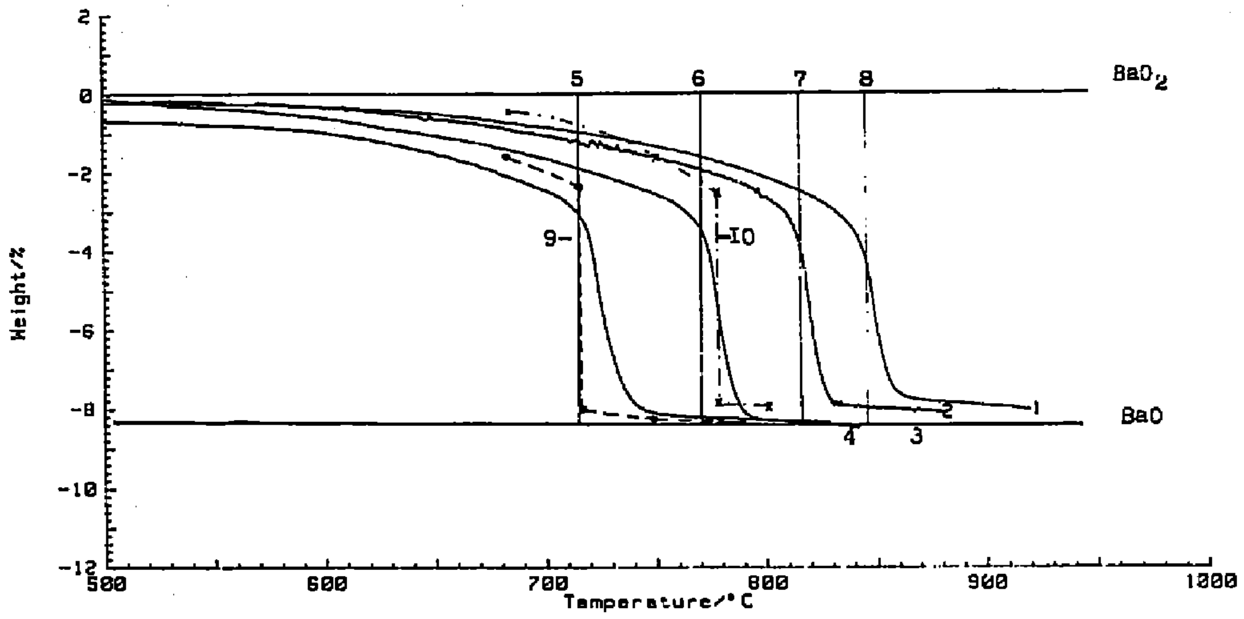

Fig. 1. Change of mass $BaO_{2.00\pm0.02}$ [$BaCO_3$(9.4 + 1.5)wt.%] versus temperature in our experiment: curve 1, 1.5 atm O_2; curve 2, 1.0 atm O_2; curve 3, 0.5 atm O_2; curve 4, 0.2 atm O_2 (ref. 6); curve 5, 0.2 atm O_2; curve 6, 0.5 atm O_2; curve 7, 1.0 atm O_2; curve 8, 1.5 atm O_2 (ref. 7); curve 9, 0.2 atm O_2; curve 10, 0.5 atm O_2.

paper [8], the possible mechanisms for oxygen incorporation in BaO were considered. In ref. 6, a conclusion concerning the appearance of the liquid phase in the BaO_2–BaO system at about 800°C was made: this was not confirmed in ref. 7.

The authors of ref. 7 suggested that the melting of BaO_2 occurred at temperatures that should be near the melting temperature of BaO ($\approx$2000°C) and at such high oxygen pressures that the decomposition of BaO_2 is prevented.

The data reported in refs. 6 and 7 are shown in Fig. 1. It is unfortunate that in ref. 6, the starting material of the experiment was the product of the decomposition of barium carbonate: as far as we know this product does not have a precise analytical formula. And in ref. 7, no information was given concerning the purity of the oxygen used in the experiment. Thus, there are some systematic discrepancies in these papers [6, 7], as well as between these results and those of our investigation where these disadvantages were eliminated.

The formal kinetic parameters of the decomposition of BaO_2 have been determined [9, 10]. The efficient activation energy (E_{act}) of the process is known to equal 191.6 kJ mol^{-1} [10]. Brunere et al. [9] list three successive steps in the reaction: embryo formation, grain growth and oxygen diffusion, their activation energies being 11.9, 104.0 and 1.66 kJ mol^{-1} respectively.

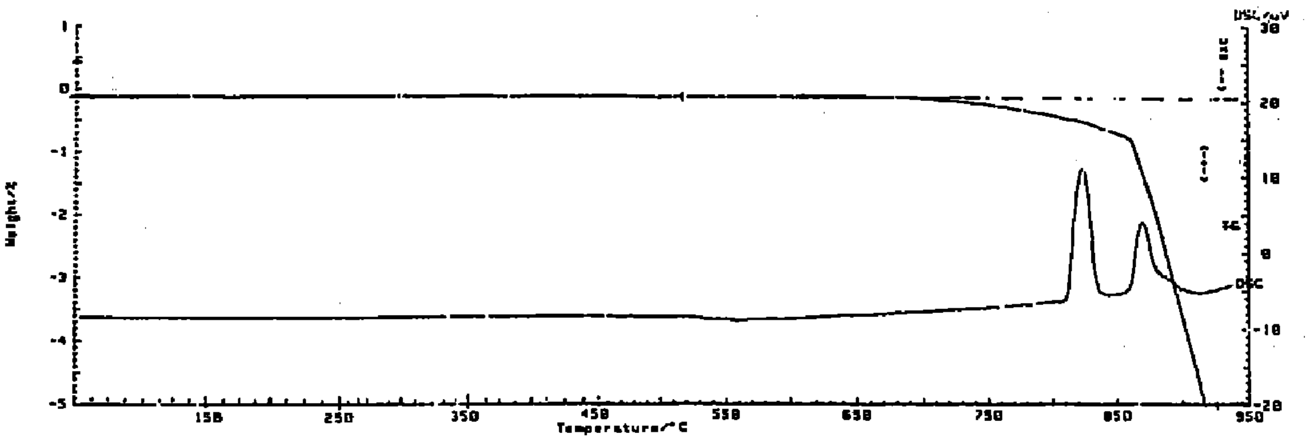

Fig. 2. Thermogram (DSC–TG) of the starting material $BaO_2 + BaCO_3$ (9.4 wt.%).

SAMPLE PREPARATION

In the present work, the starting material was thoroughly dried barium dioxide, of known barium, carbon and hydrogen content. The barium content was determined by dissolving the dried barium dixoide in a known amount of HCl. The acid excess, from which the Ba content was calculated, was titrated by trilon B. The C and H contents were determined by ignition of the starting material with chromatographic analysis of the evolving gases. The hydrogen content proved to be minimal. The composition of the starting material of this investigation was $BaO_{2.00+0.02}$ [$BaCO_3$(9.4 ± 1.5)%].

Differential thermal analysis of the barium dioxide did not show any thermal effects characteristic of compounds containing moisture or hydroxyl groups (Fig. 2). The barium carbonate used was stable over the entire temperature range of the BaO_2–BaO investigation, maintaining a constant mass up to ≈900°C. The additional experiments also show that, in a vacuum of about 10^{-4} atmospheres at 1050°C, complete decomposition of $BaCO_3$ to BaO does not take place, even following 5 hours of sintering. We believe that the kinetic discrepancies observed in the decomposition reaction of $BaCO_3$ derive from high-temperature sintering of a freshly prepared decomposition product. Therefore, barium carbonate should not be used as the starting material for the preparation and study of BaO in oxygen.

EXPERIMENTAL

The main experimental studies were carried out using a Netzsch simultaneous thermal analyser. The mass changes (Δm) were monitored continuously under a scanning mode of temperature (T) changes in an atmosphere of oxygen, previously dried over solid KOH in a steel container at a pressure of about 12 atmospheres.

A sample of optimum mass (≈30 mg) was put on to a support consisting of Al_2O_3 or MgO, the sample layer being thin to provide better contact with the gaseous medium. The temperature change rate varied over the range from 0.5 to 50°C min^{-1}. Prolonged sintering (up to 99 h) was also used.

Calibration measurements were made on empty containers before each working experiment at the relevant pressure and temperature change rate, in order to determine the buoyancy correction. Under our conditions, this correction did not exceed 1 mg up to 1500°C and is automatically taken into account in evaluating the true mass change during the continuous weighing in the course of the experiment.

The results of the experiments run using a temperature increase of 1°C min^{-1} for oxygen pressures of 0.2, 0.5, 1.0 and 1.5 atmospheres are presented in Fig. 1.

In experiments conducted at various rates of temperature change (0.5, 1.0, 5.0 and 10.0°C min^{-1}), the curves of $\Delta m(T)$ obtained by heating and cooling were practically reproducible up to temperatures that we have denoted T_{mon}. At $T > T_{mon}$, the thermogravimetric curves for heating and cooling did not coincide, i.e. hysteresis was observed.

TREATMENT AND DISCUSSION OF RESULTS

The following formula was used to calculate the oxygen index x in BaO_x from the mass change Δm

$$X = 2 - \Delta m M_{BaO_2}/0.906 m M_O$$

where $0.906m$ is the fraction of BaO_2 in the initial sample of weight m, which includes the $BaCO_3$ contaminant (9.4 wt.%), and M_{BaO_2} and M_O are the molecular weights of BaO_2 and O.

The estimated values for x (± 0.02) at various temperatures T (± 1°C) are given in Table 1 and in Fig. 3 for four oxygen pressures. Figure 4 presents a P_{O_2}–x–T diagram of part of the BaO_2–BaO system.

In order to estimate the temperature of the monovariant equilibrium more accurately, the $x(T)$ curves obtained at 1°C min^{-1} (Fig. 3, Table 1) were described by spline functions and their differentiation was performed. The points of the first extremum, $\min d^2x/dT^2$, were found on the curves. These points were taken for the temperatures of the monovariant equilibria (T_{mon}) at given pressures (Table 2).

These temperature points are connected with the appearance of a new phase, BaO. The isobars $x(T)$ (Fig. 3) obtained at $T > T_{mon}$ show a coherent coupling of the BaO and BaO_2 phases. The volume change on transformation from the structure of BaO to that of BaO_2 does not exceed the 15% that is a necessary condition for the formation of phases such as these.

The emergence of relatively strong metastable phases upon reduction

TABLE 1

The dependence of the oxygen index (x in BaO_x) on T (°C) and P_{O_2}

0.2 atm O_2		0.5 atm O_2		1 atm O_2		1.5 atm O_2		Phase composition
T	x	T	x	T	x	T	x	
500	1.89	550	2.00	500	2.00	500	2.00	$\overline{BaO_2}$
525	1.88	525	1.98	550	2.00	600	1.99	
550	1.87	550	1.97	600	1.99	700	1.93	
575	1.87	575	1.96	650	1.95	750	1.87	
600	1.85	600	1.94	700	1.90	780	1.82	
610	1.84	650	1.89	750	1.84	800	1.78	
620	1.83	700	1.82	800	1.72	810	1.75	
630	1.82	750	1.72	810	1.67	820	1.72	
640	1.81	770	1.62	812	1.64	830	1.68	
650	1.79			814	1.61	840	1.62	
660	1.79							
670	1.75							
680	1.73							
690	1.71							
700	1.68							
710	1.65							
720	1.55	772	1.61	816	1.56	842	1.6	[$BaO_2 \cdot BaO$] (metastable)
722	1.5	774	1.56	818	1.49	844	1.57	
724	1.41	776	1.5	820	1.39	846	1.52	
726	1.33	778	1.41	822	1.28	848	1.45	
728	1.26	780	1.34	824	1.21	850	1.35	
730	1.2	782	1.23	826	1.16	852	1.27	
732	1.16	784	1.17	828	1.13	854	1.21	
734	1.12	786	1.12			856	1.17	
736	1.09	788	1.09			858	1.14	
740	1.05	790	1.07			860	1.13	
745	1.03							
770	1.01	800	1.04	830	1.11	870	1.12	$\overline{BaO}$ (estimated)
795	1.00	850	1.02	840	1.10	880	1.11	
820	1.00	880	1.00	850	1.09	890	1.10	
830	1.00			870	1.09	900	1.10	
						910	1.09	

and oxidation has been investigated in detail using rare earth oxides [11, 12]. Prolonged sintering of such compounds results in complete separation of phases. In studying the components of the $BaO–BaO_2$ system, long burning at temperatures higher than T_{mon} is not possible because there is no container with which BaO does not interact in an atmosphere of dry oxygen.

In our experiments, the "substance–container" interaction was characterized by the non-reproducibility of the $\Delta m(T)$ dependence on heating

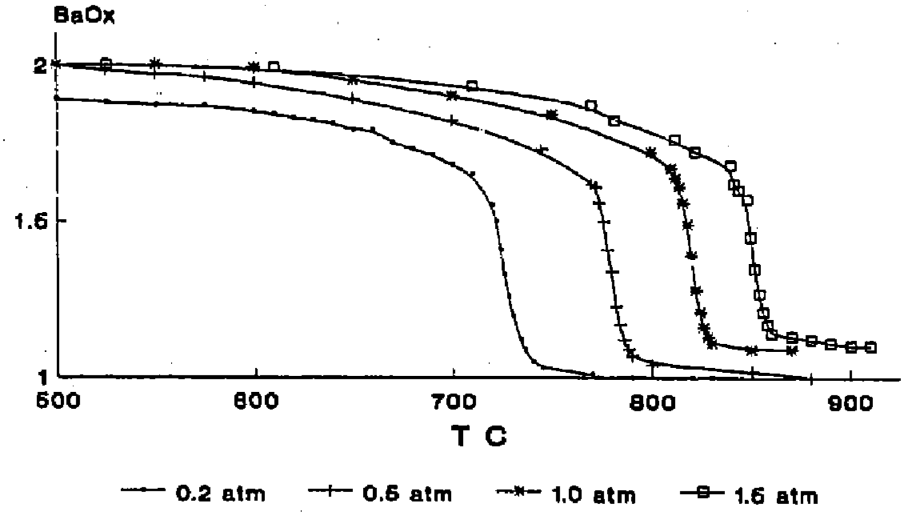

Fig. 3. The dependence of the oxygen index (x in BaO_x) on T and P_{O_2}.

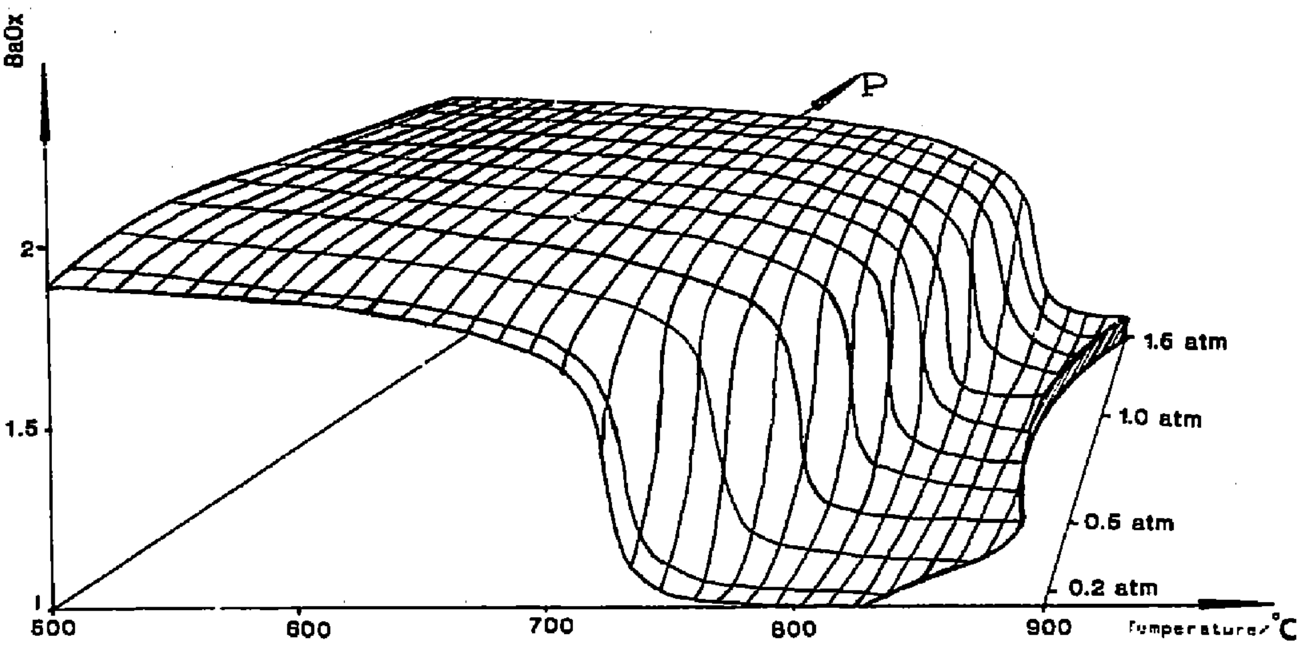

Fig. 4. Part of the space diagram P_{O_2}–x–T.

TABLE 2

Monovariant temperatures (T_{mon}) and boundary compositions of $\overline{BaO_2}$ and $\overline{BaO}$

P_{O_2} (atm)	T_{mon} (K)	$b \pm 0.02$ [a]	d [a] (estimation)
0.2	985	1.63	1.00
0.5	1043	1.62	1.04
1.0	1087	1.62	1.11
1.5	1112	1.62	1.12

[a] b and d are the oxygen indices responsible for the equilibrium boundaries of the non-stoichometric regions of BaO_2 and BaO, respectively.

higher than T_{mon} followed by cooling (hysteresis), by the increase in the container weight (≈2.0 mg) after the experiments, and by the appearance of traces of barium aluminate on the "substance–container" contact surface as detected by X-ray phase analysis.

An increase in the temperature scanning rate shifts the thermogravimetric curve towards higher temperatures in those parts of the curve where $T > T_{mon}$. With rapid temperature scanning, the equilibrium stage of the BaO_2 decomposition is not attained and the data acquired enable the activation energy (E_{act}) of the process to be estimated.

The Erofeyev's equation [13] was used for the calculations, according to which the extent of BaO_2 decomposition depends on time, in agreement with the law $\alpha = 1 - \exp(-k\tau^n)$ where $k = A\exp(-E_{act}/RT)$ is the reaction speed constant, τ is time, n is an empirical parameter (the reaction order analogue), A is a pre-exponential multiplier and R is the gas constant. The value of α was determined from experimental data using the expression

$$\alpha = 1 - [x(\tau) - d]/(b - d)$$

where $x(t)$ is the oxygen index in BaO_x at time τ, and the b and d values are given in Table 2.

For kinetic calculation we used the central portion of the isobar, $P_{O_2} = 1$ atm, data were obtained at a heating rate of $20°C\,min^{-1}$ with $T = T^*_{mon} + 20\tau$, where T^*_{mon} is the temperature of the start of BaO_2 decomposition.

After transformations, Erofeyev's equation has the form

$$U = \ln(-\ln(x - d)/(b - d)) - n\ln(T - T^*_{mon})/20 = \ln A - E_{act}/RT$$

It was assumed that $n = 1$ because only in this case is the function $U(1/T)$ satisfactorily described by a linear dependence. As a result of calculations, we obtained

$$E_{act} = \partial U/\partial(1/T) = 360 \pm 20\ (\mathrm{kJ\,mol^{-1}})$$

It is believed that the limiting stage of BaO_2 decomposition is associated with the formation and growth of the new phase (embryo formation).

The thermogravimetric data obtained were applied to evaluate the thermodynamic properties of the system in question. As can be seen in Fig. 3, the curve $x(T)$ can be divided into three parts. The first and the third parts characterize an equilibrium of the type

$$1/\delta BaO_x + 0.5 \rightarrow 1/\delta BaO_{x+\delta}; \quad \delta \rightarrow 0$$

BaO_x lies in the $\overline{BaO}$ or $\overline{BaO_2}$ regions.

The excess chemical potential of oxygen in these regions can be

TABLE 3

Coefficients of the approximations of eqn. (1)

	w_{00}	w_{01}	w_{10}	w_{11}	w_{20}	w_{21}
$\overline{BaO_2}$	−2362763	644.4856	−670253.4	3611.087	3917975	−5489.927
$\overline{BaO}$	−27.0926E7	21193.46	7.756E7	−61026.72	−7.4573E7	59111.84

represented by some mathematical surfaces

$$\mu_O^{ex} = (1-n)^2[w_{00} + w_{01}T + 2n(w_{10} + w_{11}T) + 3n^2(w_{20} + w_{21}T)] \quad (1)$$

where $n = x/(1+x)$ is the mole fraction of oxygen. The coefficients (see Table 3) were determined using a special program developed in the Laboratory of Chemical Thermodynamics of the MSU.

The estimation of the Gibbs energy change for equilibrium

$$1/(b-d)BaO_d + 0.5O_2 = 1/(b-d)BaO_b$$

was made from the data of Table 2

$$\Delta G_2^\ominus = -72.44 + 66.72 \times 10^{-3}T\ (\pm 2\%) \quad (2)$$

To determine the Gibbs energy of the reaction

$$BaO_{1.0} + 0.5O_2 = BaO_{2.0} \quad (3)$$

the approximation equations $\Delta\mu(x, T)$, eqn. (1), were integrated for the bivariant regions $\overline{BaO}$ and $\overline{BaO_2}$, and combined with $\Delta G_2^\ominus$ for the monovariant region. To obtain $\Delta_f G^\ominus(BaO_2)$, literature data were used for $\Delta_f G^\ominus[BaO]$ [14]. The results of the estimation are presented in Table 4 and Fig. 5.

Comparison with the literature data shows that the discrepancy in the temperature of BaO_2 decomposition does not exceed 9 K, but the

TABLE 4

Thermodynamics functions

T (K)	$\Delta G_2^\ominus(\pm 2\%)$ (kJ (g at. O)$^{-1}$)	$\Delta G_3^\ominus$ (kJ (g at. O)$^{-1}$) estimated	$\Delta_f G^\ominus(BaO_2)$ (kJ mol^{-1})	
			This work	Ref. 4
985.5	−6.70	−5.1	−460.5	−462.8
1043	−2.83	−2.05	−452.4	−452.9
1087	0	0.34	−445.7	−445.4
1112	1.77	1.74	−441.7	−441.0

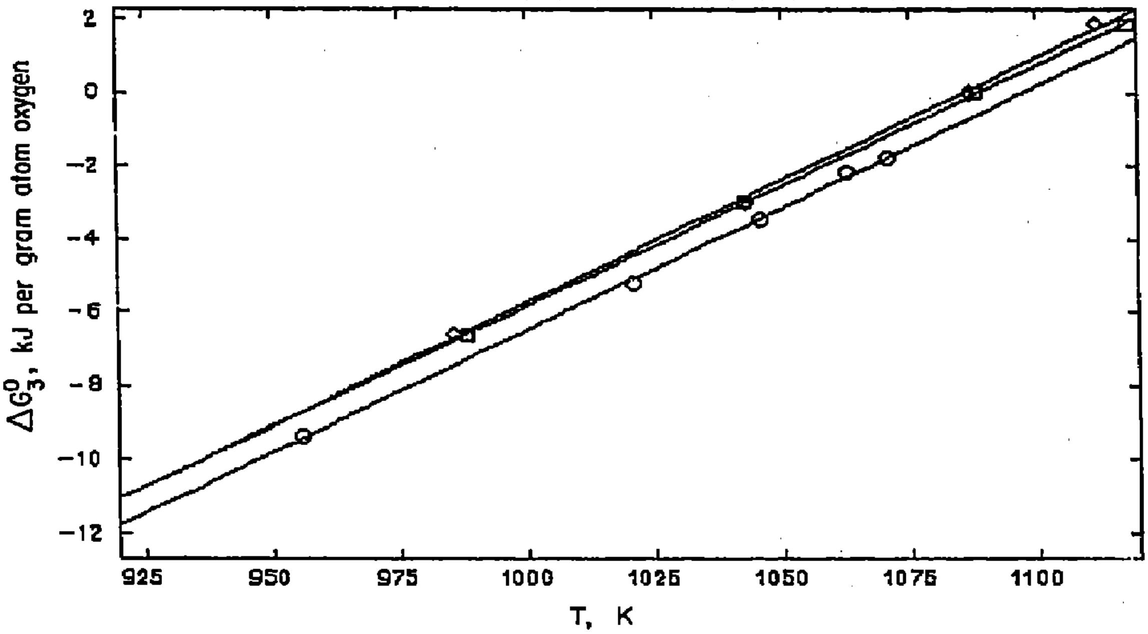

Fig. 5. Dependence of Gibbs energy on temperature for the reaction $BaO + 0.5O_2 = BaO_2$: ◇, this work; ○, ref. 6; □, ref. 7.

discrepancy in the boundaries of the non-stoichometric regions is considerable. Nevertheless, this does not significantly affect the values of $\Delta_r G^{\ominus}(BaO_2)$ [14].

REFERENCES

1 J.H. Hildebrand, J. Am. Chem. Soc., 34 (1912) 250.
2 G.M. Lewis and M. Randall, J. Am. Chem. Soc., 36 (1914) 1986.
3 A. Blumental, J. Chim. Phys. Phys. Chim. Biol., 34 (1937) 633.
4 M.M. Pavlucenko and Ja.S. Rubincik, Russ. J. Phys. Chem., 33 (1958) 849.
5 I.I. Volnov, Peroxides of Alkali Earth Elements, Nauka, Moscow, 1983, p. 12.
6 O.V. Kedrovski, P.V. Kovtunenko, E.V. Kiseleva and A.A. Bundel, Russ. J. Phys. Chem., 41 (1967) 414.
7 I.L. Aptekar, A.V. Kosenko, A.A. Gohov, V.M. Masalov and G.A. Emelcenko, Superconductivity: Phys. Chem. Eng. (Rus.), 4 (1991) 801.
8 P.V. Kovtunenko and Ja. L. Harif, Usp. Khimii, (Rus.), 48 (1979) 448.
9 V.Ja. Brunere and A.N. Dokucaeva, Iz. Akad. Nauk. Latvijskoj SSR, Serija Chimiceskaja, No. 3 (1990) 332.
10 B.V. Erofeev and N.D. Sokolova, Tables for Calculations on Topokinetic Equation $\alpha = 1 - \exp(-kt^n)$, Akad. Nauk BSSR, Minsk, 1963, p. 3.
11 J. Kordis and L. Eyring, J. Phys. Chem., 72 (1968) 2030, 2044.
12 L. Eyring, J. Solid State Chem., 1 (1970), 376.
13 A.Ja. Rosovski, Heterogeneous Chemical Reactions, Nauka, Moscow, 1980, p. 320.
14 S.A. Degterov and G.F. Voronin, Superconductivity: Phys. Chem. Eng. (Rus.), 4 (1991) 1758.